AMMRC CTR 77-26

AD

MACHINE CASTING OF FERROUS ALLOYS

October 1977

R. Mehrabian, S.D.E. Ramati, G.J. Abbaschian, D.G. Backman
Y.V. Murty

Department of Metallurgy and Mining Engineering
Department of Mechanical and Industrial Engineering
University of Illinois at Urbana-Champaign
Urbana, IL 61801

Prepared for

ARMY MATERIALS AND MECHANICS RESEARCH CENTER
Watertown, Massachusetts 02172

AMMRC CTR 77-26

MACHINE CASTING OF FERROUS ALLOYS

R. Mehrabian, D. G. Backman, G. J. Abbaschian,
Y. V. Murty, and S. D. E. Ramati

Department of Metallurgy and Mining Engineering
Department of Mechanical and Industrial Engineering
University of Illinois at Urbana-Champaign
Urbana, IL 61801

D D C

MAR 2 1978

F
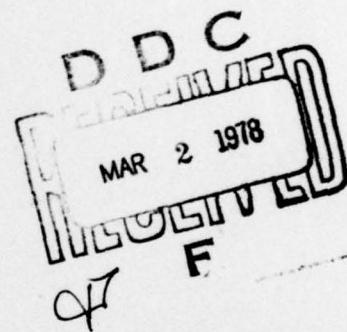
DISTRIBUTION STATEMENT A
Approved for public release;
Distribution Unlimited

FOREWORD

TABLE OF CONTENTS

I. INTRODUCTION

This report is the third describing work carried out at the University of Illinois at Urbana-Champaign as a part of a joint university-industry research program on machine casting of ferrous alloys. Work at the University of Illinois was initiated on 1 October 1975; at that time, the overall program had already been in effect for 33 months. The initial aim of the program was to plan and test new and innovative processes and develop a machine casting system for ferrous alloys that would produce good quality parts economically and at high speed.

Emphasis of the work at the University of Illinois is on processes and casting systems which employ a partially solid alloy as charge material. The program at the University of Illinois is especially designed to establish the processing conditions necessary to produce porosity-free parts and to evaluate the Rheocasting and Thixocasting processes from both a technical and an economical point of view.

During the first year of this investigation [1,2]*, work was carried out in the following areas:

1. A variety of casting systems were designed, constructed, and operated; these include the following:

    (a) A transparent model continuous slurry producer,

    (b) A low-temperature alloy continuous slurry producer and a direct chill assembly that permits production of Rheocast ingots semi-continuously,

---

*Numbers in brackets refer to entries in REFERENCES.

    (c) A high-temperature alloy continuous slurry pro-

      ducer, and

    (d) A laboratory casting machine which permits direct

      observation and photography of mold filling.

  2. The important relationships between process variables

    and the structure of continuously produced partially

    solidified slurries were studied.

  3. The relationships between gating systems, process

    variables, and mold filling characteristics of differ-

    ent viscosity materials were studied in the trans-

    parent casting machine.

  4. Initial work was carried out to determine the heat

    treatment response and mechanical properties of high-

    temperature alloys.

  5. A cost analysis model was developed to permit economic

    evaluation of the new machine casting process.

This semi-annual report covers work carried out in the past six months on two of the topics listed above (items 2 and 4) and summarizes all the important findings in these two areas in the past 18 months.

II. THE EFFECT OF PROCESS VARIABLES ON THE STRUCTURE OF A PARTIALLY SOLIDIFIED SLURRY

In a number of papers published in the past few years the practical applications of a new metal forming process, Rheocasting, were described [3-5]. Fundamental aspects of the process relating structure of a partially solidified, vigorously agitated, Sn-15%Pb alloy to its rheological behavior were studied in a high temperature viscometer [6]. The work described herein is a continuation of this latter study carried out on a continuous slurry production apparatus. This apparatus was specifically designed to permit close control of process variables during partial solidification. General relationships are developed between process variables during slurry production and the structure of the primary solid particles.

Earlier work carried out on a high temperature viscometer [6] has shown that the structure and rheological behavior of a Sn-15%Pb alloy slurry are a function of three process variables. These variables are: the average shear and cooling rates during primary solidification and the volume fraction of solid in the slurry.

The general trends established relating process variables to the structure and the viscosity of the metal slurries were:

(a) Increasing the average shear rate generally reduces the amount of entrapped liquid in the solid particles resulting in a corresponding decrease in viscosity. Shear rate also affects the size of the primary particles at slow cooling rates--primary solid particle size decreases with increasing average shear rate.

(b) Increasing the average cooling rate during primary solidification reduces the size of the primary solid particles, but increases

the amount of entrapped liquid--increases the effective volume
fraction of solid in the slurry, hence increases its viscosity.

(c) As the volume fraction solid in a slurry increases, so does
its viscosity.

(d) For a given average shear and cooling rate, the relative vis-
cosity* of a partially solid metal slurry, η_r, at volume fractions
solid larger than ~ 0.2, can be described by an exponential equation,

$$\eta_r = A \exp Bg_s \tag{1}$$

where A and B are constants depending on average shear and cooling
rates, and g_s is volume fraction solid.

(e) Metal slurries are thixotropic (their viscosity decreases with
increasing rate of shear, is time dependent and reversible) and
show a hysteresis loop phenomenon similar to other well known thixo-
tropic systems. Measured areas of hysteresis loops (a quantitative
measure of thixotropy) increase with increasing volume fraction
solid, initial viscosity and time at rest.

(f) Relative viscosities of partially solidified metal slurries
are: (i) 1 to 2 orders of magnitude higher than suspensions of non-
interacting spheres of polystyrene, rubber latex, glass and methyl-
methacrylate, and (ii) of the same order of magnitude as suspensions
of interacting particles like Kaolin (clay) in water. The high vis-
cosity of the latter suspension has been explained on the basis of
an aggregation mechanism [8]. A similar mechanism has been proposed

---

*The relative viscosity of a suspension is defined as $\eta_r = \eta_a/\eta_o$
where η_a is apparent viscosity of the suspension and η_o is the
viscosity of the liquid.

for the interacting solid particles in a metal slurry [6]. Figure
1 shows data obtained for the slurries of an Sn-15%Pb alloy over a
wide range of thermomechanical treatments, as well as reported data
for the nonmetallic systems noted above.

1. Apparatus

The basic design and operation of a similar apparatus used
for production of high temperature alloy slurries have previously
been reported [1,2]. A schematic illustration and photograph of
the low temperature system used in this study are shown in Figures
2 and 3. It consists of a multiple chamber stainless steel crucible
and associated heating and cooling systems and a mixing assembly.
The temperature of each chamber is individually controlled by auto-
matically regulating the power and coolant inputs to a series of
heating and cooling coils located along the crucible length. This
control enables alteration of the thermal process parameter. In a
portion of this work a controlled temperature hot oil cooling system
was used around the lower mixing chamber, Figure 2. During opera-
tion, the temperature gradient in this chamber is measured via the
five thermocouples located along its length.

The mixing mechanism previously described [1,2] provides vigorous
agitation within the lower (mixing) chamber. The rotor in the present
system is made of stainless steel with a square cross section,
0.025m x 0.025m. Rotation speed can be varied between 0 to 1600 RPM.

The flow of the slurry through the system is controlled by adjusting the distance between the rotor bottom and the exit port valve seat. Sn-Pb stock is continuously fed to the top chamber either in liquid or solid form. Production rates in this system can be varied between $2x10^{-3}$ to $20x10^{-3}$ Kg/sec depending on the heating and cooling rates used in the lower mixing and partial solidification chamber. The exiting slurries are either directly water quenched or chill cast using the mold described below.

The direct chill casting assembly located below the continuous slurry producer is schematically illustrated in Figure 2. The mold is made of graphite with a slightly tapered cylindrical hole located in its center. The top half of the mold is heated with controlled resistance heating coils while the bottom half is water cooled. This arrangement coupled with vibration of the mold assembly permits production of smooth surface ingots with slurries containing volume fractions of primary solid as high as ~ 0.5. Finally, a water spray is directed on the ingot as it is withdrawn from the graphite mold by the pedestal and the withdrawal assembly. A photograph of an Sn-15%Pb ingot produced in this way is shown in Figure 3.

2. Process Variables

The three important process variables in the continuous slurry producer affecting structure are average shear and cooling rates and volume fraction solid.

(a) <u>Average shear rate</u>. The average shear rate is a function of the rotor geometry, the clearance between the rotor and the lower mixing chamber, and the rotation speed. The following equation gives the average shear rate in the annulus in the mixing chamber.

$$\dot{\gamma}_{Ave} = \frac{2\Omega_o}{(1-\kappa^2)} \kappa \tag{2}$$

where $\dot{\gamma}_{Ave}$ equals the average shear rate, Ω_o is angular velocity and κ is defined as:

$$\kappa = \frac{\text{perimeter of the square rotor}}{\text{perimeter of the mixing chamber}}$$

In the machine of Figures 2 and 3, the value of κ is 0.86 and at a rotation speed of 1000 RPM the calculated average shear rate $\dot{\gamma}_{Ave} = 692 \text{ sec}^{-1}$.

(b) <u>Average cooling rate</u>. The average cooling rate is a function of the thermal profile within the mixing chamber including the temperature and volume fraction of solid of the discharged slurry. The average cooling rate in the mixing chamber is defined by the following equation:

$$\varepsilon_{Ave} = \frac{\Delta T_s(g_s)}{t_f} \tag{3}$$

where g_s is the volume fraction of primary solid particles in the slurry, $\Delta T_s(g_s)$ is the difference between the liquidus temperature and the temperature of the exiting slurry, and t_f is the residence time of the alloy in the mixing chamber while in the solidification range. Figure 4 shows a set of curves of average cooling rate versus average flow rate calculated from measured thermal data, flow rates and equation (3).

(c) <u>Volume fraction solid</u>. The volume fraction solid of primary spheroidal solid particles in the exiting slurry is dependent on the rate of heat withdrawal in the mixing chamber, the rate of material flow through the chamber, and the physical properties of the metal produced. Once the temperature in the mixing chamber at the exit port has been determined, the volume fraction of solid can be calculated. For the binary Sn-15%Pb alloy, in which the densities of the liquid and the solid are not too different, volume fraction solid and weight fraction solid are approximately equivalent, and the Scheil equation is used.

$$g_s = 1 - \left[\frac{T_M - T_L}{T_M - T}\right]^{1/1-k} \tag{4}$$

where T_M is the melting point of the pure tin, T_L is the liquidus temperature of the alloy and T is the actual temperature in the liquid-solid range.

3. Results

Results of this work on continuously produced slurries confirm earlier findings [6] that average cooling rate during primary solidification has the most pronounced effect on the size of the primary solid particles. Therefore, a corollary program was carried out to compare these structures with conventional dendritic structures solidified under identical average cooling rates.

Figure 5 shows data obtained from a large number of experiments carried out in the slurry producer, as well as dendrite arm

spacings of conventional casting solidified over a range of temperatures. Average primary solid particle size, p.p.s., in a slurry measured via standard quantitative techniques, decreases with increasing average cooling rate. This observation is not only in line with results obtained from the dendritically solidified castings, but our results indicate that the size of the particles in a slurry is approximately equivalent to the primary dendrite arm spacings in the conventional castings solidified under identical cooling rates. The dashed line in Figure 5 is for the partially solidified slurries-- it was drawn using least mean square of the data. Representative structures of a conventionally solidified and continuously processed slurry are shown in Figure 6. The photomicrographs in Figure 7 show the effect of increased average cooling rate during primary solidification on the fineness of structure of the slurries.

Figure 8 shows the effect of cooling rate on size distribution of the primary solid particles. The size frequency and cumulative percent were determined on polished cross-sections of water quenched specimens. At the lower average cooling rate, $\varepsilon = 0.61°C/sec$, the distribution is rather broad -- the ratio of standard deviation to average particle size, $\sigma/\overline{X}$, is 0.38. The size distribution of primary solid particles decreases with increasing cooling rate. At the average cooling rate of $\varepsilon = 5.57°C/sec$ the values of $\sigma/\overline{X}$ is 0.31. This finding is contrary to that reported earlier [6]. However, the range of cooling rates used in the earlier work was much lower, 0.005 to 0.42°C/sec. As indicated below the effect of shear rate on particle size and distribution is more pronounced at low cooling

rates and this probably contributed to the discrepancy between the two sets of results.

Changes in average shear rate affect the size of the primary particles only at low cooling rates. Figures 9 and 10 show this effect on average particle size and size distribution, respectively. The largest particles measured in the top 15% of the cumulative curve are denoted as LPPS in Figure 9. Data in this figure show that increasing the cooling rate reduces the size of the primary solid particles. Furthermore, supportive data in Figure 10 show that the particles become more uniform in size as the average shear rate is increased from 100 to 1360 sec^{-1}. The corresponding calculated values of $\sigma/\overline{X}$ are 0.64 and 0.31, respectively. The photomicrographs in Figure 11 show the effect of increased shear rate on structure. It was also noted that the amount of entrapped liquid in the primary solid particles increases with increasing cooling rate and decreasing shear rate. These findings are in line with those reported earlier in experiments carried out in a high temperature viscometer [6].

Finally, large changes in volume fraction solid, for example from 0.2 to 0.6, result in a corresponding increase in primary solid particle size. However, over the smaller volume fraction solid ranges (0.4 to 0.6 for the data shown in Figure 6) the effect of cooling rate is much more pronounced.

III.   SEGREGATION, HOMOGENIZATION HEAT TREATMENT, AND MECHANICAL PROPERTIES OF RHEOCAST ALLOYS

In general, engineering alloys freeze over a range of temperatures and liquid concentrations. As a consequence, the different elements that are combined to make up an alloy segregate during solidification. Short range segregation (microsegregation) occurs on the dendritic scale in conventional castings. One may thus anticipate a similar segregation phenomenon in Rheocast metals. Microsegregation spacings in Rheocast metals would be on the scale of the primary solid particles when the slurry is slowly solidified in a mold resulting in an essentially equiaxed structure. On the other hand, if the slurry is rapidly solidified, as in die casting, the remaining liquid solidifies in a dendritic mode and a duplex microstructure is obtained--the primary solid particles are surrounded by a fine dendritic network.

The important influence of dendrite arm spacings on the mechanical properties of conventional castings, and of wrought material produced from conventionally cast ingots, is well documented. Large improvements in mechanical properties can also result from high temperature "homogenization" treatments. Whether the time necessary to obtain significant homogeneity is short enough to be commercially feasible depends on the spacings over which concentration differences occur. As noted in the previous section, both dendrite arm spacings in conventional castings and primary solid particle size in Rheocast slurries decrease with increasing average cooling rate during solidification. Thus, one would expect that, regardless of differences in microsegregation profiles between dendritic and Rheocast alloys, the finest primary

solid particle size should give the shortest response to "homogenization" heat treatment.

Application of Rheocast technology to specific commercial forming and casting processes would be realized once the full range of static and dynamic properties of a number of Rheocast alloys are documented. In the 18 months, a comprehensive study was initiated at the University of Illinois to determine the effect of cast (Rheocast) structure on microsegregation, homogenization heat treatment response and mechanical properties of several high temperature alloys. Results from this work are presented below. It should be noted that the measured properties reported were obtained from static ingots cast using the high temperature continuous Rheocasting machine previously described [2].

1. Structure of Rheocast Alloys

The three alloys studied were 905 copper base alloy (Cu-10%Sn-2%Zn), 440C stainless steel (Fe-17%Cr-1%Mn-1%Si-0.6%C) and X-40 cobalt base superalloy (Co-26.5%Cr-10.5%Ni-7%W-0.5%C). Typical Rheocast (water quenched) structures of two of the alloys are shown in Figure 12. For comparison, Figure 12 also shows the corresponding conventionally solidified dendritic structures of the alloys. As previously noted, the primary solid particle size in the Rheocast alloys is primarily a function of average cooling rate during solidification. Therefore, processing techniques that can increase cooling rate during continuous Rheocasting and yet permit solidification of spheroidal

primary solid particles could become of foremost importance in the future.

An example of this relationship is shown in Fig. 13 where the dendrite arm spacings for conventionally cast X-40 cobalt base alloy and the primary particle size for partially solid X-40 alloy are plotted versus the average cooling rate during solidification. For the conventionally solidified material the relationship between dendrite spacing and cooling rate can be described by the following equations:

$$d = 90\varepsilon^{-0.32} \text{ primary} \tag{5}$$

$$d = 40.4\varepsilon^{-0.27} \text{ secondary} \tag{6}$$

where d represents the dendrite spacing and ε is the average cooling rate during solidification. Also, as can be observed in Fig. 13, the primary particle size is close to that of primary dendrite spacings obtained at equivalent cooling rates.

The structure of Rheocast ingots of the 440C stainless steel and the X-40 cobalt base superalloy are shown in Figure 14. Due to the slower cooling rates achieved in the insulated molds (1 1/4" in diameter by 7" high) the ingots do not show the typical duplex structure of the water quenched slurries. The primary solid particles coarsen during solidification in the ingot molds resulting in an equiaxed austenitic structure delineated by coarse intergranular carbides. For the 440C stainless steel alloy the carbides are of the form M_7C_3 whereas for X-40 cobalt base superalloy several carbides are reported to form upon solidification including M_7C_3, $M_{23}C_6$, and M_6C [9]. The strong

carbide forming elements present in X-40, tungsten and chromium, participate predominantly in carbide formation although the carbides dissolve small percentages of the cobalt present. A typical chemistry for $M_{23}C_6$ carbides in cobalt base superalloys is $Cr_{18}Co_4W_1C_6$ [9].

(a) Microsegregation

As previously noted, solute elements are redistributed during the solidification of engineering alloys producing microsegregation. In order to determine the extent of solute segregation, conventionally cast and Rheocast X-40 alloys were analyzed with an electron microprobe. Analysis of water quenched slurries consistently showed flat elemental composition profiles of alloying elements in the primary solid particles with abrupt changes at their boundaries. An example of this observation in the X-40 cobalt base superalloy is snown in Figure 15. This segregation profile differs from conventional dendritic microsegregation where a minimum or maximum concentration is usually observed at the center of dendrite arms. The composition profiles for the X-40 dendritic microstructure are shown in Fig. 16. The electron probe microanalysis of both dendritic and Rheocast X-40 show that in each case chromium and tungsten segregate in a positive manner with a maximum concentration in the interdendritic or interparticle region. Nickel segregates in the opposite manner. A quantitative explanation of the segregation phenomena occurring during the solidification of partially solid alloys will be presented in a subsequent section.

2. Microsegregation, Heat Treatment Response, and Properties

Ingots of the three alloys were subjected to different homogenization heat treatments and their mechanical properties were determined. The effect of heat treatment for each alloy is to dissolve non-equilibrium phases present between primary solid particles and to provide a more homogeneous distribution of solute elements within the grains. The heat treatments adopted in each case is equivalent to practice used for conventionally solidified dendritic material. Each alloy system will be described separately below.

(a) Copper Base Alloy 905

Ingots of copper base alloy 905 were subjected to homogenization heat treatment at 770°C for 20 hours. Following treatment standard tensile specimens of the material were tested in tension using an Instron testing machine. In order to gauge the effect of homogenization heat treatment, samples were also tested in the as-Rheocast condition. The room temperature properties of 905 copper base alloy are listed in Table I. The properties obtained are comparable to conventionally solidified dendritic castings. During homogenization, however, the yield strength increased whereas both the ultimate tensile strength (UTS) and the percentage elongation decreased. The decrease of the latter two properties is probably the result of coarsened porosity following homogenization heat treatment.

(b) Stainless Steel, 440C

Rheocast ingots of 440C stainless steel were homogenized at 1100°C to 1300°C for times of up to 20 hours. Compression test specimens

from these ingots were subjected to standard 400C alloy quench and temper heat treatment. The specimens were tested at different temperatures up to 600°C. It was found that 0.2 percent offset yield strength improved with increasing time and temperature of homogenization heat treatment, Figure 17. For example, the room temperature yield strength of the as-Rheocast material was approximately 150 KSI. After five hours at 1300°C, the measured yield strength increased to approximately 240 KSI. This value is close to the 270 KSI reported for wrought 440C. Improvement in the yield strength of the as-Rheocast alloy with homogenization heat treatment is a direct consequence of transformation of the grain boundary M_7C_3 carbides to $M_{23}C_6$ carbides. This conversion is accompanied by the diffusion of carbon and homogeneous redistribution of the latter carbides within the equiaxed grains of the alloy [10].

(c) Cobalt Base Superalloy--X-40

High temperature homogenization treatments were conducted at 1100°C and 1300°C in a vacuum of 6×10^{-5} mm of Hg for a period of 5 hours. Subsequently the samples were furnace cooled. A portion of the samples were aged at 770°C for 50 hours and water quenched following homogenization. The microstructure obtained in the as Rheocast and homogenization heat treated conditions is shown in Fig. 18. In addition the homogenized structures were analyzed with the electron microprobe. An example of the results is shown in Figure 19 where the concentration profiles of chromium, nickel, and tungsten are plotted versus position for a sample homogenized for five hours at 1300°C.

During homogenization the interparticle carbide network dissolves producing a source of solute atom which diffuses into the grain bulk. This process, given sufficient time, goes to completion for homogenization temperatures in excess of approximately 1150°C [9]. Below this temperature a small equilibrium volume fraction of primary carbides remain at the grain boundary. Evidence of these effects are shown in Fig. 18 where comparison of heat treated and as-Rheocast specimens show that there is a dramatic decrease in the volume fraction of intergranular carbides. Also, by comparing the composition profiles measured before and after homogenization, Figs. 15 and 19, the increase in concentration of the carbide forming elements, chromium and tungsten, within the grain interior is readily apparent following heat treatment.

During slow cooling from the homogenization temperature, as was necessary with the available Brew vacuum furnace, carbides reprecipitate within the grain bulk in the form $M_{23}C_6$. The precipitate initially develops as fine particles around the outer periphery of the grain (Fig. 18b). During aging treatment, as in service use, the precipitate coarsens. Room temperature monotonic tensile properties were measured using an Instron with a pin loaded specimen employing 0.75" strain gauge and with a cross head speed of 0.2 in/min. The results are compared with reported conventional investment cast properties and design minimum in Table II. While the yield strengths of the investment cast and Rheocast materials are equivalent, the ductility and the ultimate tensile strength of Rheocast ingots are lower. Metallographic examination showed that the lower ductilities are due to extensive microporosity in the Rheocast ingots. The high volume

fraction of the slurry and lack of directional solidification were responsible for the observed microporosity. To further analyze the effect of porosity, ingots of X-40 were hot isostatically pressed at 1200°C and 15,000 psi and stress rupture tested at 790°C with a tensile stress of 30 KSI. As noted in Table II the stress rupture properties of the Rheocast ingots are comparable to investment casting and exceed the minimum design requirements in aircraft components.

The high temperature mechanical properties of Rheocast material was evaluated by compression tests at different temperatures and measuring the 0.2% yield strength, Fig. 20. It was also necessary to conduct tests on dendritic material whose primary dendrite arm spacings is close to the primary particle spacing of the Rheocast material for comparison. The Rheocast and aged X-40 cobalt base alloy exhibited yield strength higher than its dendritic counterpart up to he test temperature of 400°C. After 1100°C homogenization treatment followed by aging, the yield strength dropped considerably. This degradation of properties could be attributed to redistribution of primary carbides by coarsening and attendant changes in their chemistry [10].

Detailed microhardness measurements were carried out across the primary solid particles of as-Rheocast and heat treated specimens using a 25 gram load, Figure 21. The carbide/primary solid particle interface has been denoted as the edge of the grain and the KHN is normalized by taking the ratio of hardness at a given location to the minimum value which consistently occurred at the center of the pri-

mary solid particles. In the as-Rheocast condition the microhardness inside the primary solid particles exhibited no change complementing the microprobe analysis of Figure 15. Heat treatment for five hours at 1100°C and 1300°C increased the relative hardness in the particles significantly, Figure 21. Dissolution of grain boundary carbides, solute redistribution, and reprecipitation of fine carbides during furnace cooling after heat treatment as described previously are responsible for the changes in relative microhardness.

The results reported above show that Rheocast ingots respond to heat treatment and in the absence of porosity possess mechanical properties comparable to conventional casting. Therefore, as in conventional processes, variables during Rheocasting and subsequent casting or forming operations should be closely controlled to obtain sound components.

IV.   REFERENCES

1. Mehrabian, R., D. G. Backman, Y. V. Murty, R. J. Lauf, S. D. E. Ramati, and S. Hong, "Machine Casting of Ferrous Alloys," Semi-annual Technical Report, ARPA Contract No. DAAG46-76-C-0023, 1 October to 31 March 1976, prepared for Army Materials and Mechanics Research Center, Watertown, Mass.

2. Mehrabian, R., D. G. Backman, Y. V. Murty, G. J. Abbaschian, S. D. E. Ramati, S. Hong, and R. J. Lauf, "Machine Casting of Ferrous Alloys," Semi-annual Technical Report, ARPA Contract No. DAAG46-76-C-0023, 1 April 1976 to 30 September 1976, prepared for Army Materials and Mechanics Research Center, Watertown, Mass.

3. Flemings, M. C. and R. Mehrabian, Trans. AFS, Vol. 81, 1973, p. 81.

4. Riek, R. G., A. Vrachnos, K. P. Young, N. Matsumoto, and R. Mehrabian, Trans. AFS, Vol. 83, 1975, p. 25.

5. Mehrabian, R. and M. C. Flemings, "New Trends in Materials Processing," Proc., American Society for Metals, 1976, p. 98.

6. Joly, P. A. and R. Mehrabian, J. of Materials Science, Vol. 11, 1976, p. 1393.

7. Thomas, D. G., J. Colloid Sci., Vol. 20, 1965, p. 267.

8. Michaels, A. S. and J. C. Bolger, I.E.C. Fundamentals, Vol. 1, No. 3, August 1962, p. 153.

9. Sims, C. T. and W. C. Hagel, Super Alloys, John Wiley and Sons, New York, 1972, pp. 145-174.

10. Oblak, J. M. and W. H. Rand, "Structure and Properties of the Rheocast Ferrous Alloy 44C," Metallurgical Trans., Series B, Vol. 7B, 1976, p. 705.

11. Standard Handbook, Cast Copper and Copper Alloy Products, Copper Development Association, Inc., New York, 1970, p. 106.

TABLE I

Mechanical Properties of Copper Base Alloy 905

	YS (KSI)	UTS (KSI)	% Elongation
As Rheocast	19	47	30
Rheocast and Homogenized at 770°C for 20 hours	22.6	44.3	23
Conventional Dendritic Alloy*	22	45	25

*Typical mechanical properties of commercial conventionally cast 905 alloy reported in Ref. 11.

TABLE II

Mechanical Properties of X-40 Cobalt Base Alloy

Property	As-Rheocast	Investment Cast	Design Minimum
0.2% Tensile Yield Strength (KSI)	77	76	50
Ultimate Tensile Strength (KSI)	96	108	83
% Elongation	3.0	7	4.0
Stress-Rupture at 790°C and 30 KSI following isostatic pressuring at 1200°C and 15,000 psi	58.6	60	--
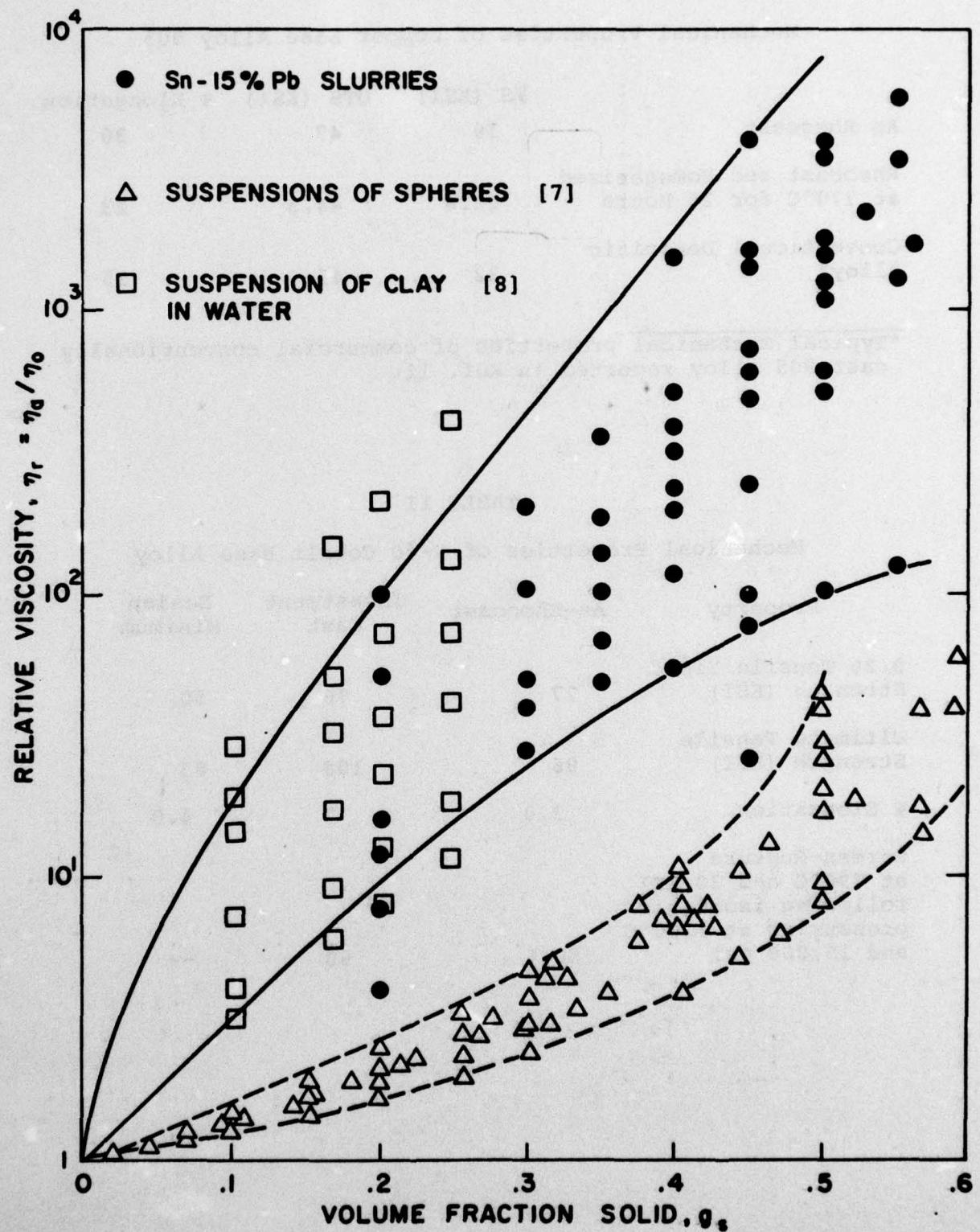
Figure 1. Comparison of the relative viscosity of Sn-15%Pb slurries to that of other suspensions of interacting and non-interacting particles. From reference (4).
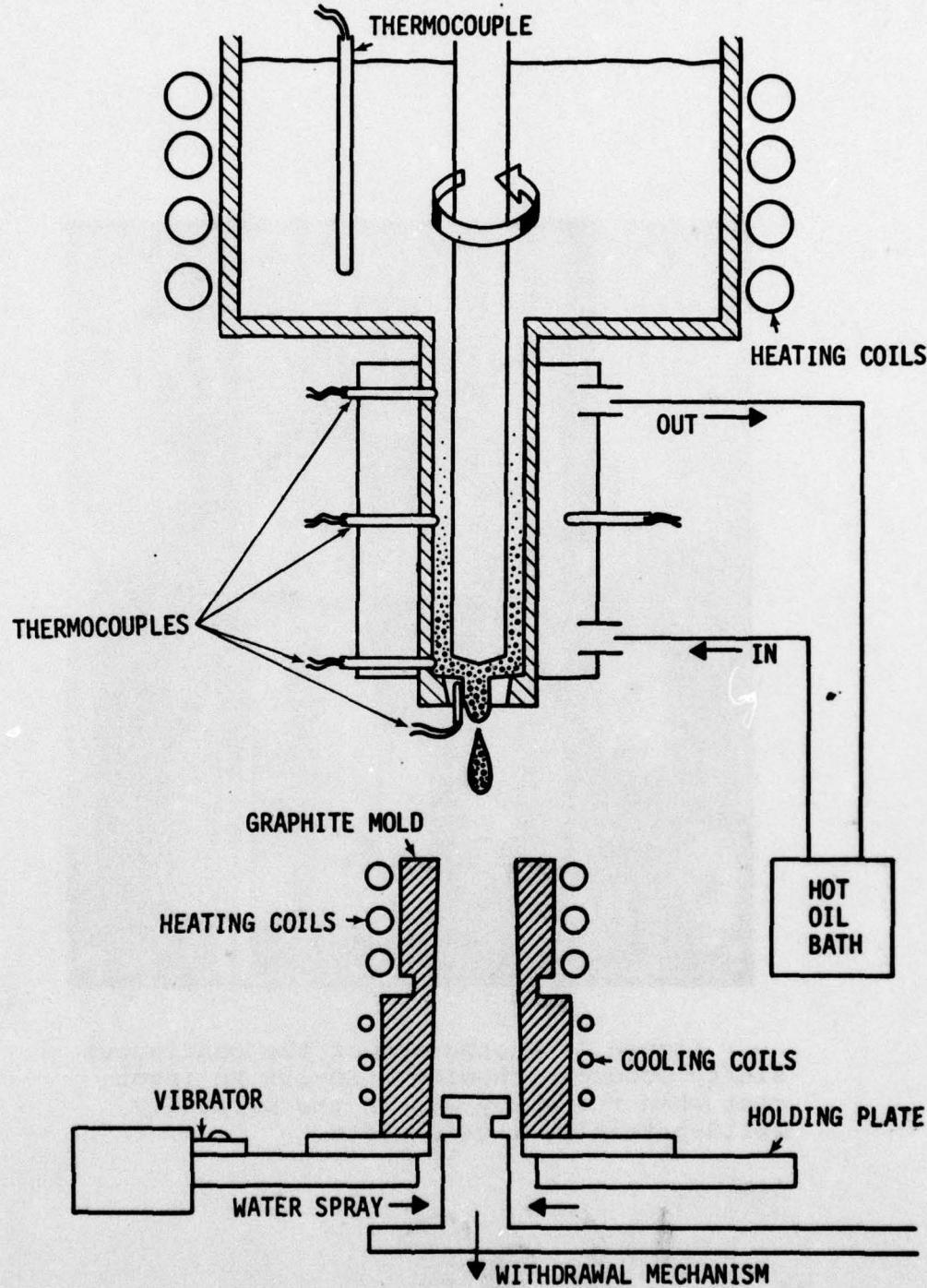
Figure 2. Schematic illustration of the continuous slurry producer and associated mold arrangement for direct chill casting of semi-continuous ingots.
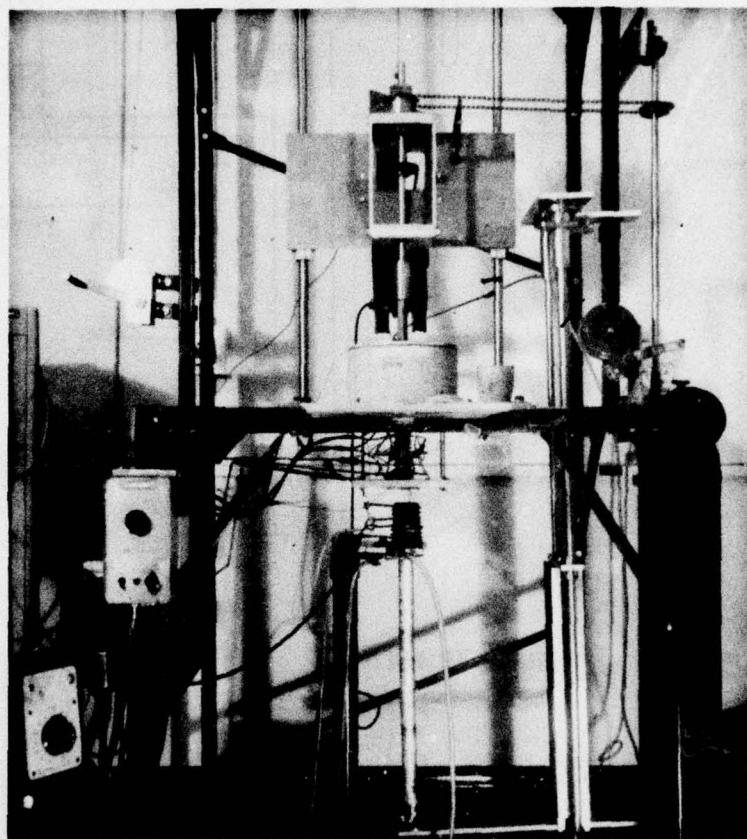
Figure 3 Photograph of the continuous
slurry producer showing a Sn-15% Pb ingot
cast when the alloy was in the partially
solid-partially liquid state.
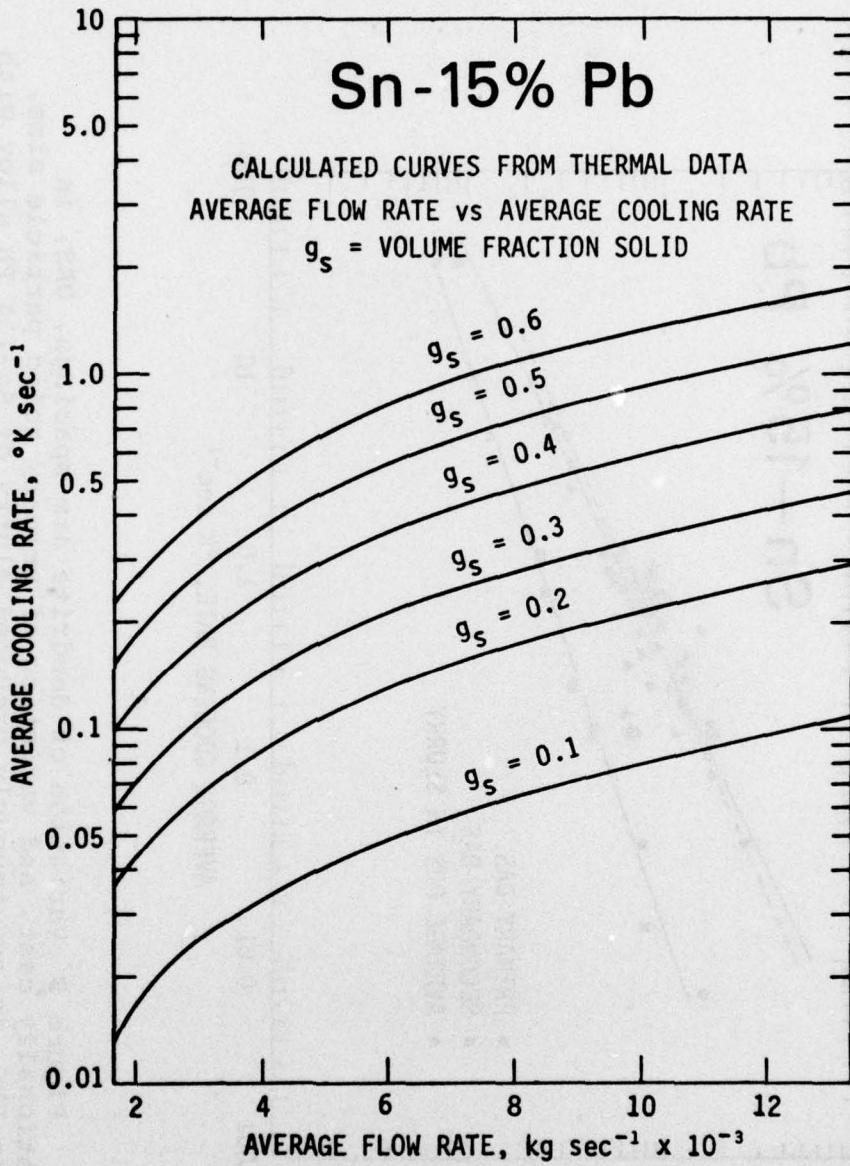
Figure 4 Cooling rate versus flow rate
at different volume fractions solid determined
using actual thermal measurements made in the
continuous slurry producer.
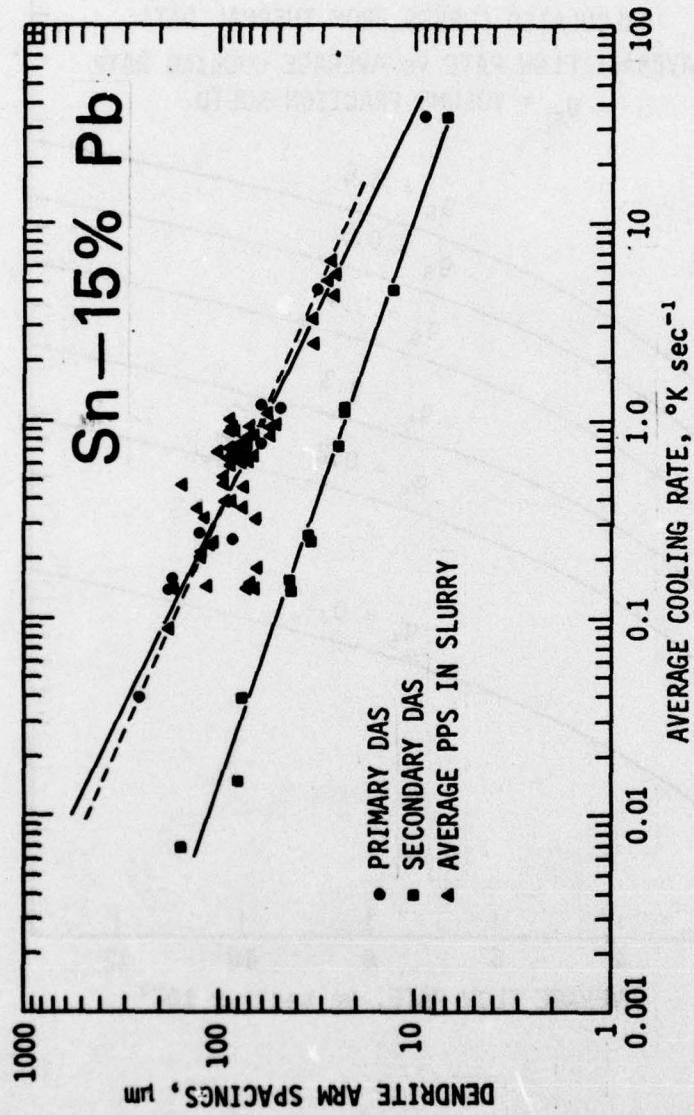
Figure 5 Variation of dendrite arm spacings, DAS, in conventionally cast, and variation of primary solid particle size, average PPS, in continuously produced slurry of Sn-15% Pb alloy with cooling rate during solidification.
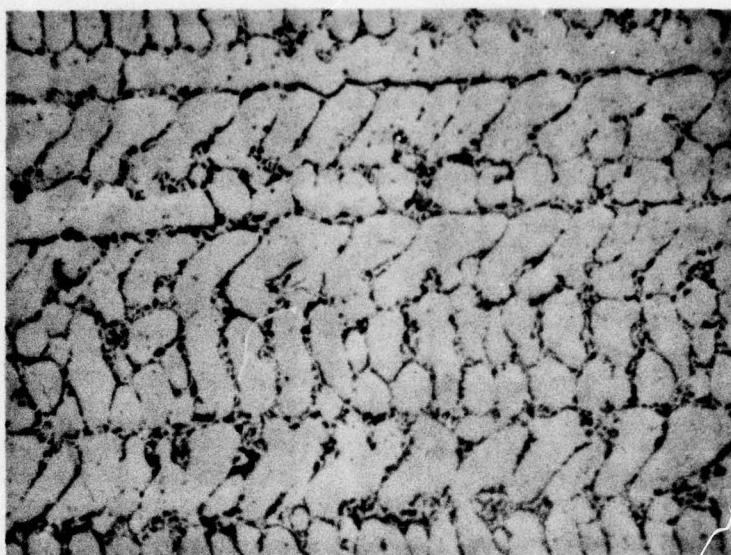
[a]
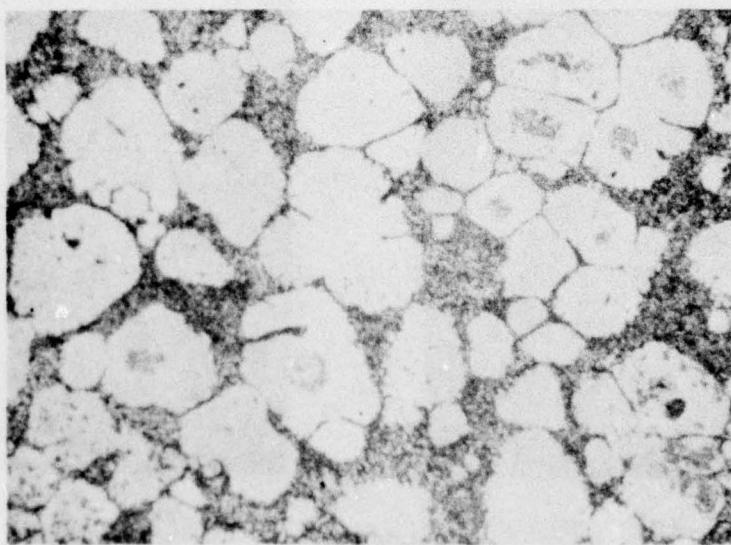
[b]

Figure 6 Microstructures of conventionally solidified (dendritic) and continuously produced slurry of Sn-15% Pb alloy. Cooling rate during solidification of both specimens was ∿1°K·sec^{-1}; (a) conventionally solidified dendritic structure, (b) slurry structure, shear rate and volume fraction solid were 420 sec^{-1} and 0.6, respectively, 250X.
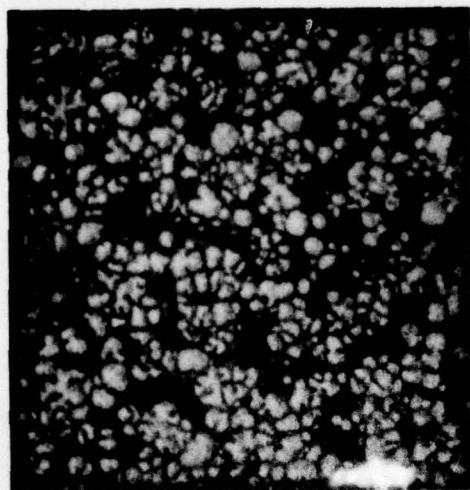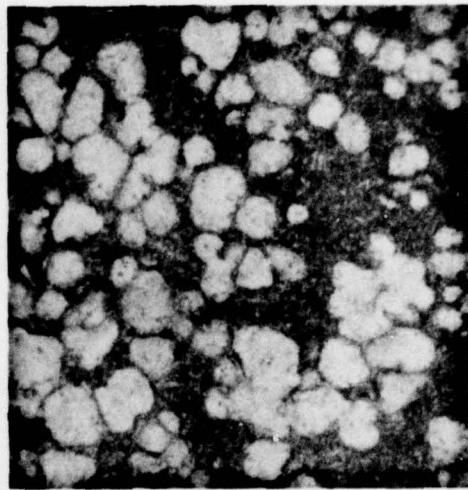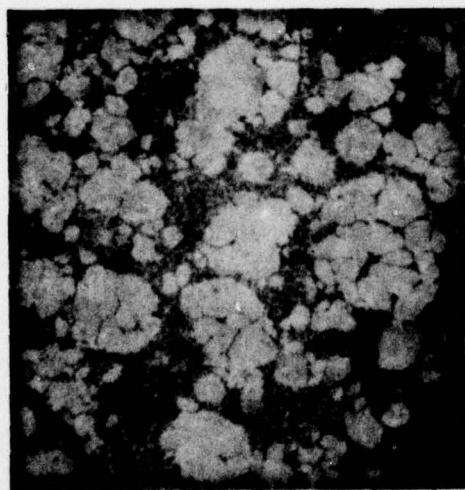
Figure 7 Effect of cooling rate, at a given shear rate ∿650 sec^{-1}, on the structure of continuously produced slurries of Sn-15% Pb alloy; (a) and (b) cooling rate was 5.52°K·sec^{-1}, 100X and 250X, respectively; (c) and (d) cooling rate was ∿0.87°K·sec^{-1}, 100X and 250X, respectively.
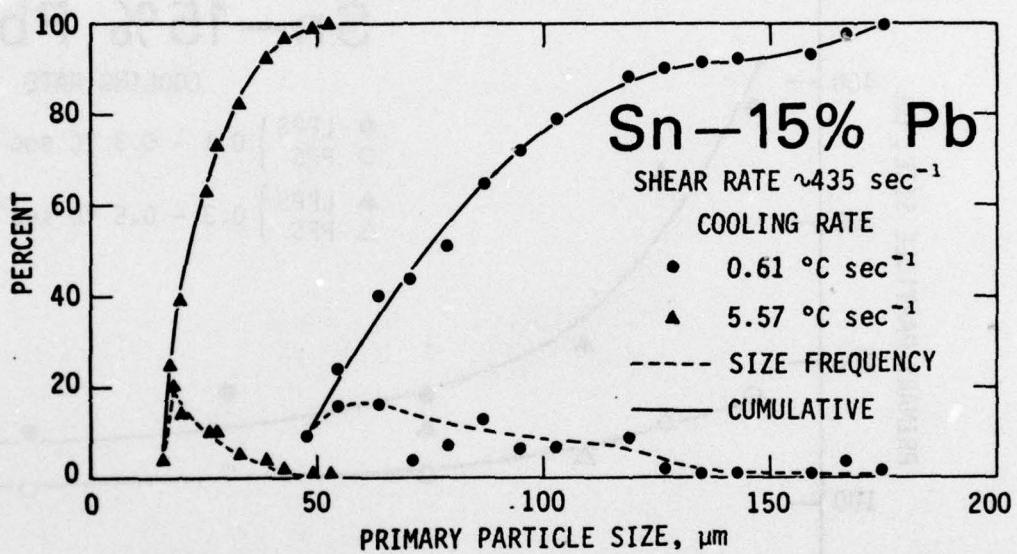
Figure 8. Effect of cooling rate, at a given shear rate of ~435 sec⁻¹, on percent size frequency and cumulative percent of primary solid particles in continuously produced slurries of Sn-15%Pb alloy.
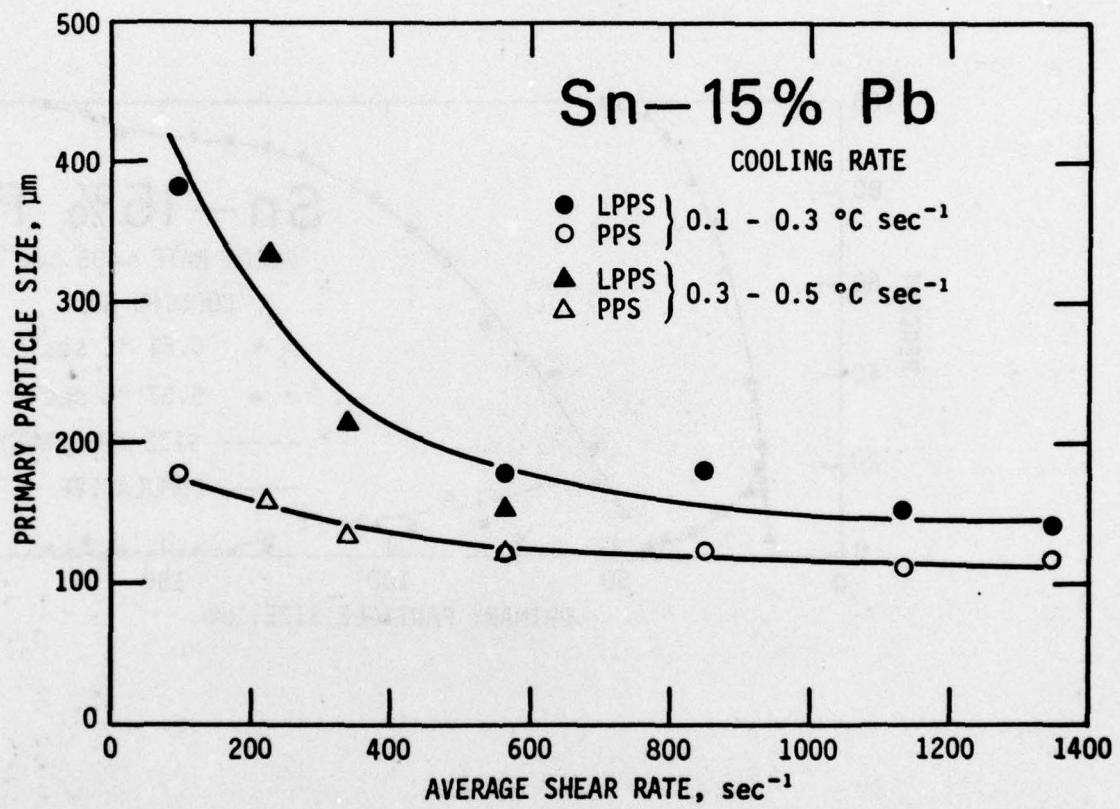
Figure 9. Variation of primary solid particle size in continously produced slurries of Sn-15%Pb alloy with shear rate at cooling rates of 0.1 to 0.5°K.sec⁻¹.
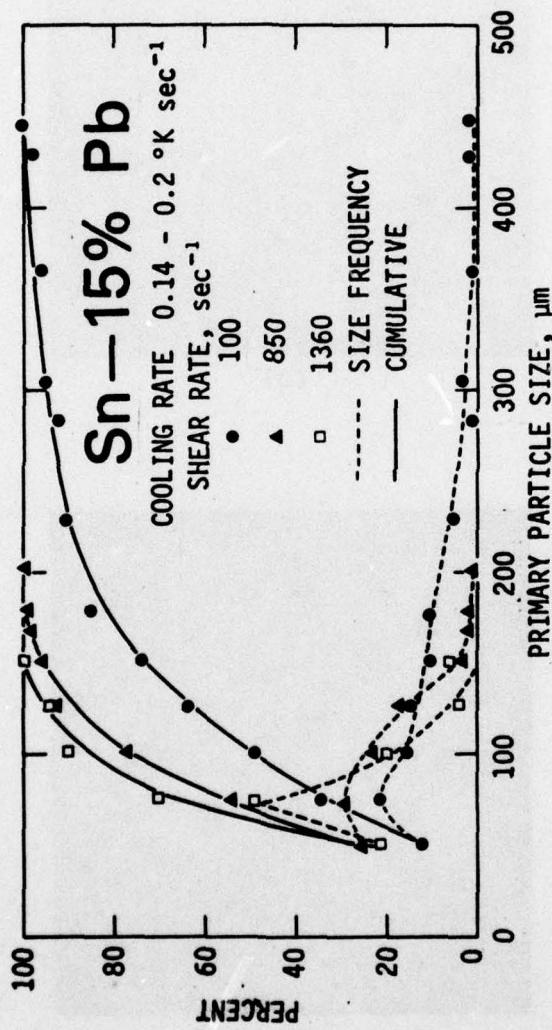
Figure 10 Effect of shear rate, at cooling rates of
~0.14 to 0.2°K·sec⁻¹, on percent size frequency and cumu-
lative percent of primary solid particles in continuously
produced slurries of Sn-15%Pb alloy.
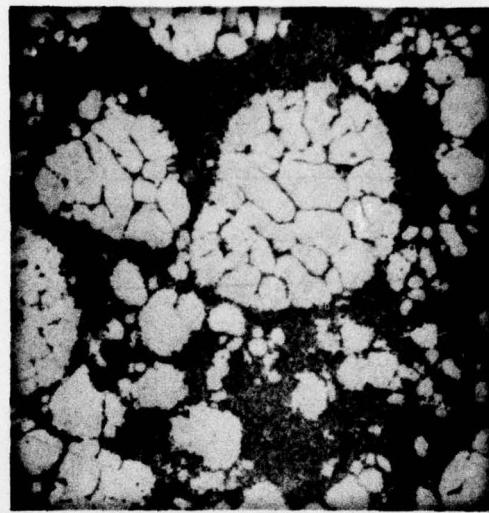
(a)
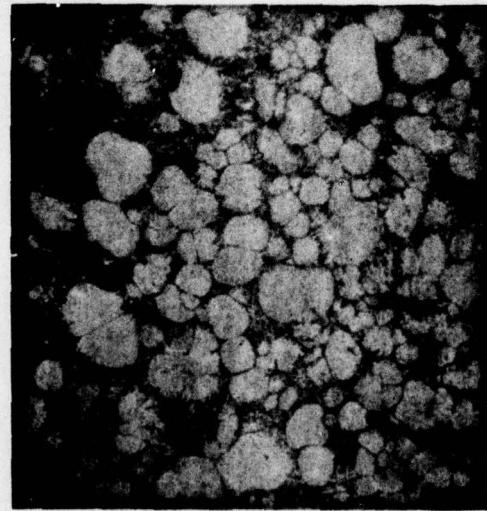
(b)

Figure 11   Effect of shear rate at low cooling rate
$\sim 0.14°K^{-1}$ on the structure of continuously produced slurries
of Sn-15% Pb alloy; (a) shear rate was 100 sec^{-1}, (b) shear
rate was 1360 sec^{-1}, 100X.
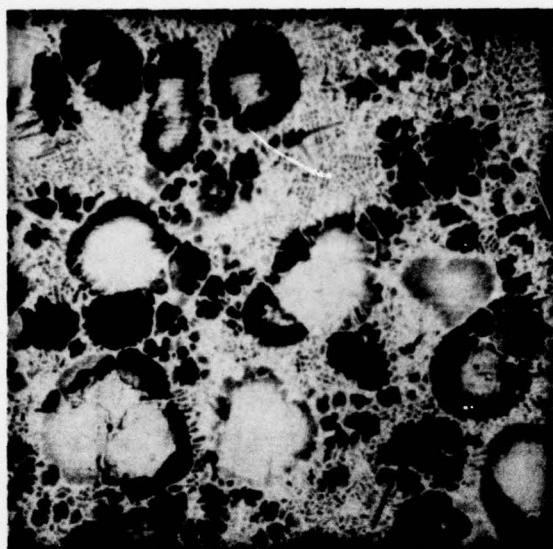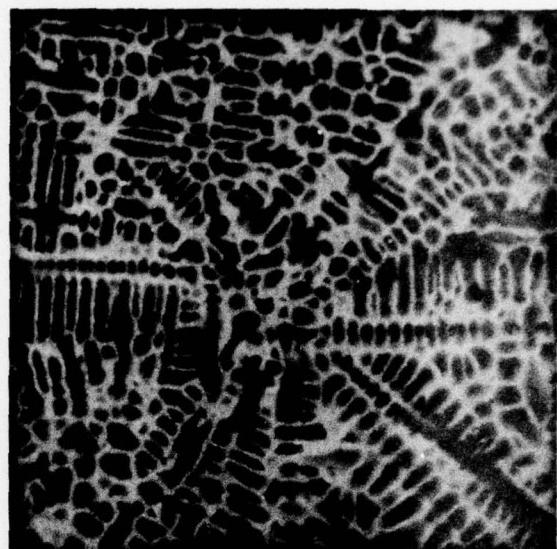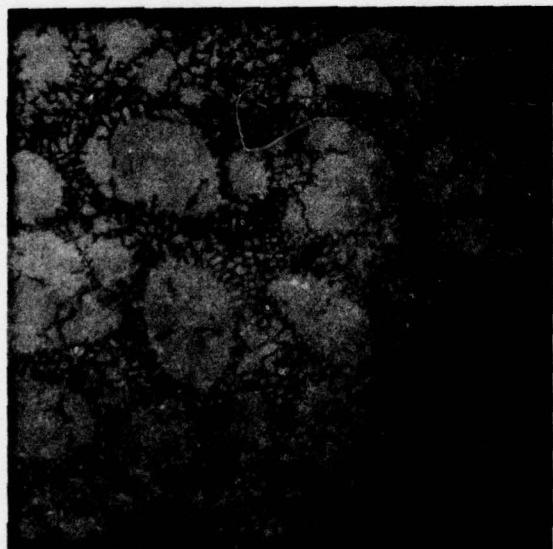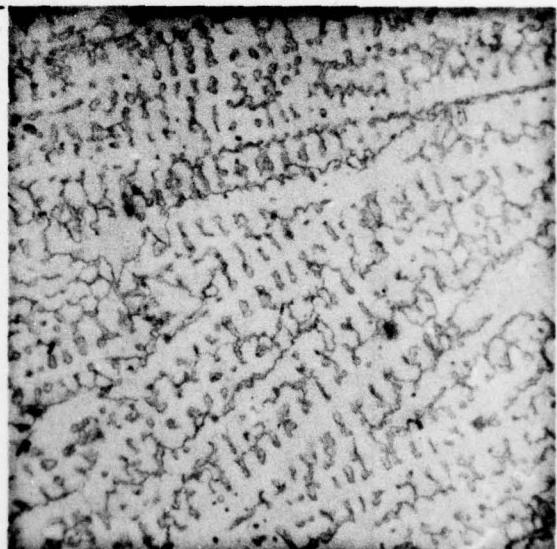
Figure 12 Comparison of Rheocast and conventionally cast (dendritic) microstructures of high temperature alloys solidified at equivalent cooing rates: (a) and (b) show the Rheocast and conventional dendritic microstructures of 440C stainless steel, respectively; (c) and (d) show the Rheocast and conventional dendritic microstructures of X-40 cobalt base superalloy, resepctively. Magnification 100X.
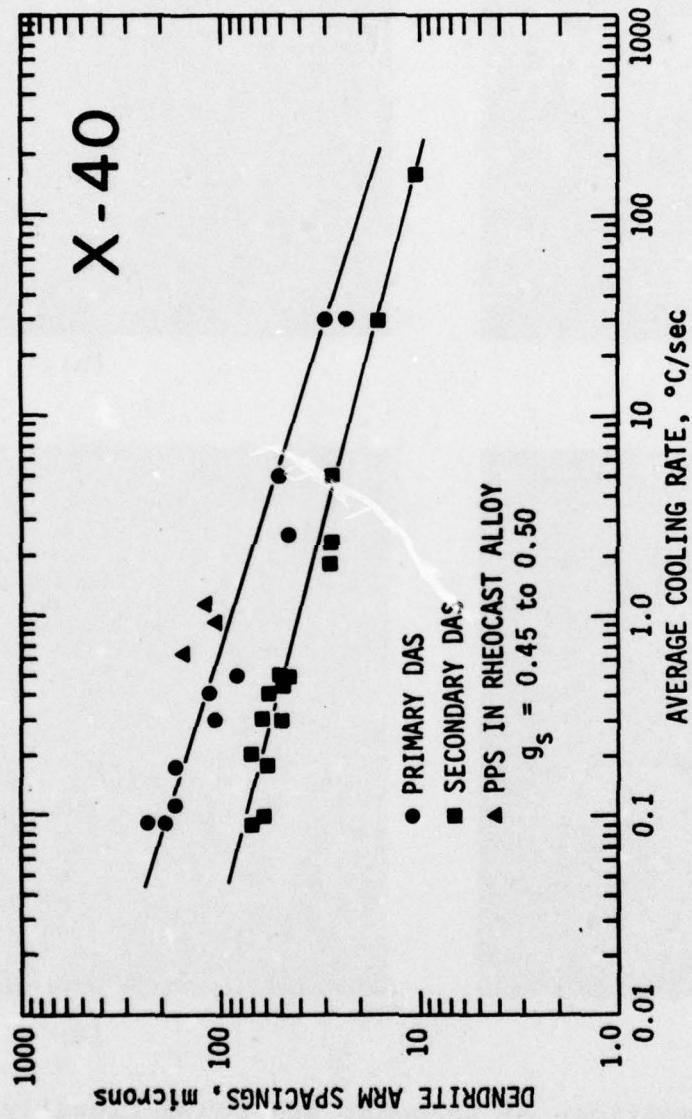
Figure 13 Variation of dendrite arm spacings, DAS, in con-
ventionally cast, and variation of primary solid particle size, P.P.S.,
in continuously produced slurry of X-40 cobalt base superalloy with
average cooling rate during solidification.

(a)

(b)

Figure 14   Ingot microstructures of continuously
produced semi-solid alloy; (a) 440C stainless steel
and (b) X-40 cobalt base superalloy.   Samples were
slowly cooled in ingot molds.   Magnification 65X.
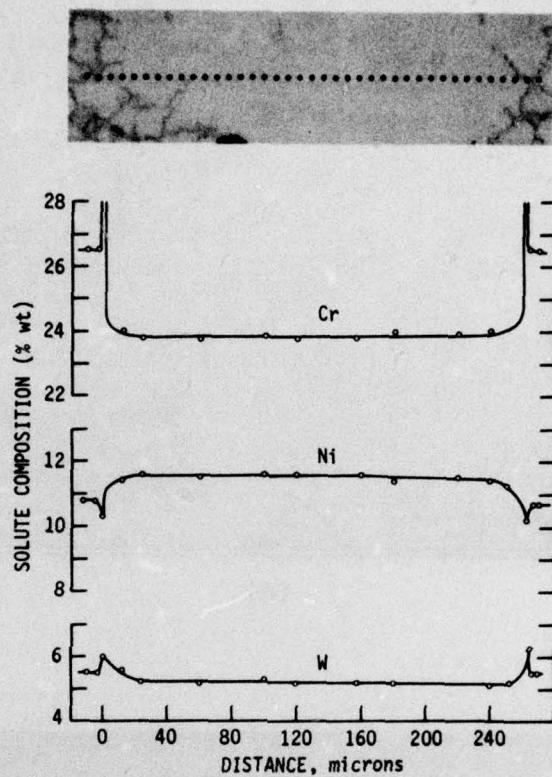
Figure 15 Composite figure showing microprobe
trace and photograph of microstructure of Rheocast X-40
cobalt base superalloy. Solute distribution is along
dotted path shown in the photograph. Both the graph and
the photograph have the same scale in the horizontal
direction.
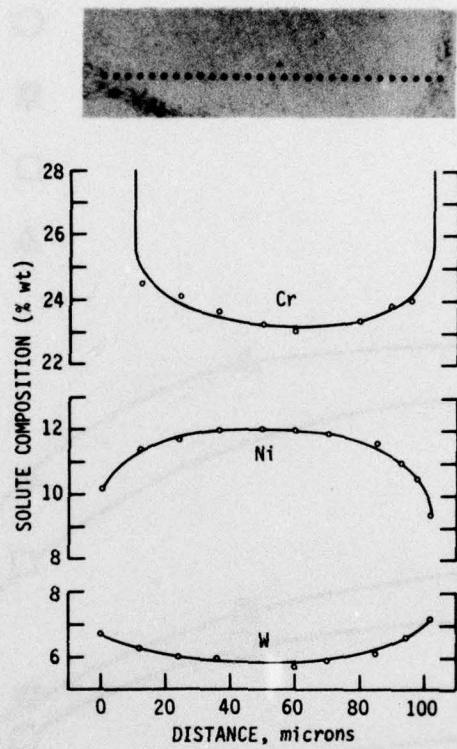
Figure 16 Composite figure showing microprobe trace
and photomicrograph of conventionally solidified, dendrite,
X-40 cobalt case superalloy. Solute distribution is along
dotted path shown in the photograph. Both the graph and
the photograph have the same scale in the horizontal direction.
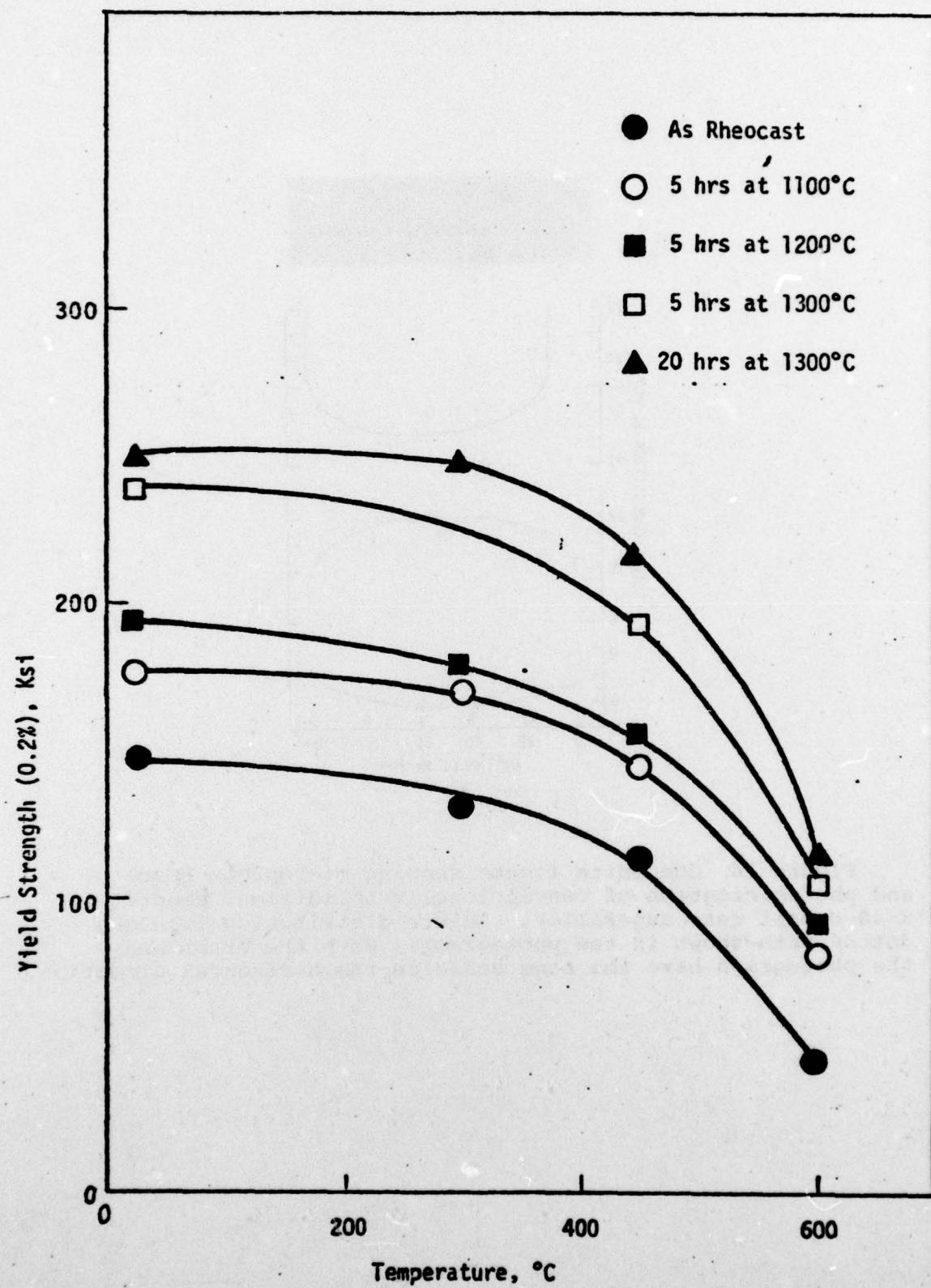
Figure 17 Measured compressive yield strength of as-Rheocast
and homogenization heat treated 440C stainless steel as a function
of temperature.

(a)　　　　(b)　　　　(c)
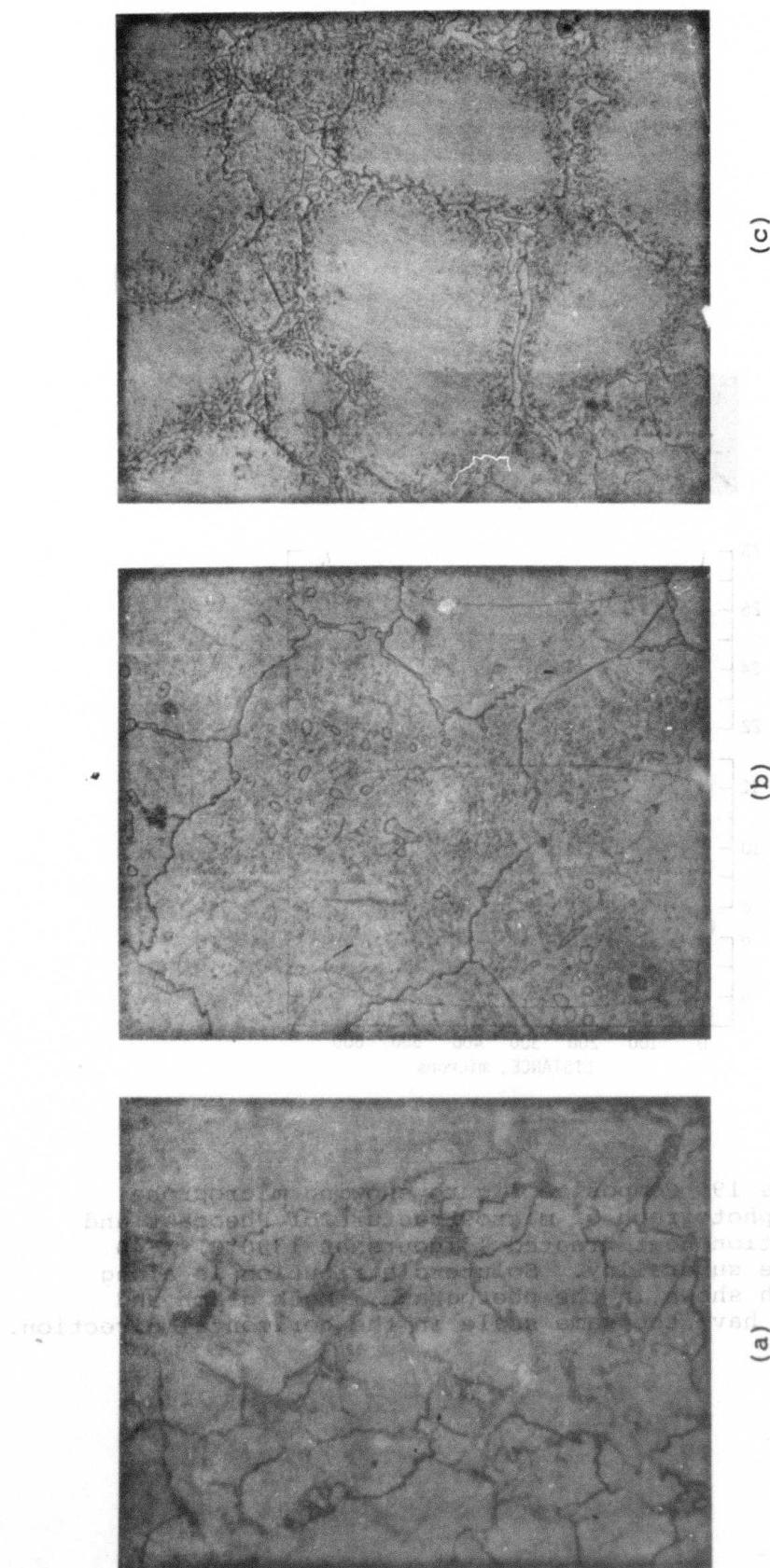
Figure 18 Photomicrographs of ingot microstructures of X-40 cobalt base alloy, magnification 400X. (a) as Rheocast; (b) and (c) homogenized 5 hours at 1100 and 1300°C, respectively.
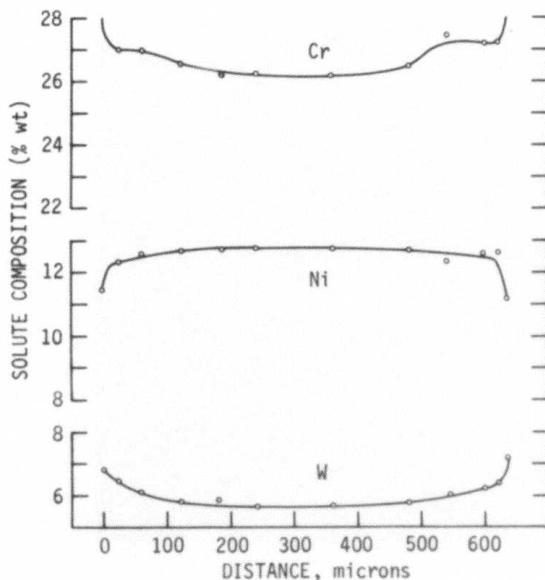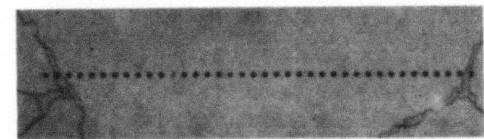
Figure 19   Composite figure showing microprobe trace and photograph of microstructure of Rheocast and homogenization heat treated (5 hours at 1300°C) X-40 cobalt base superalloy.   Solute distribution is along dotted path shown in the photograph.   Both graph and photograph have the same scale in the horizontal direction.
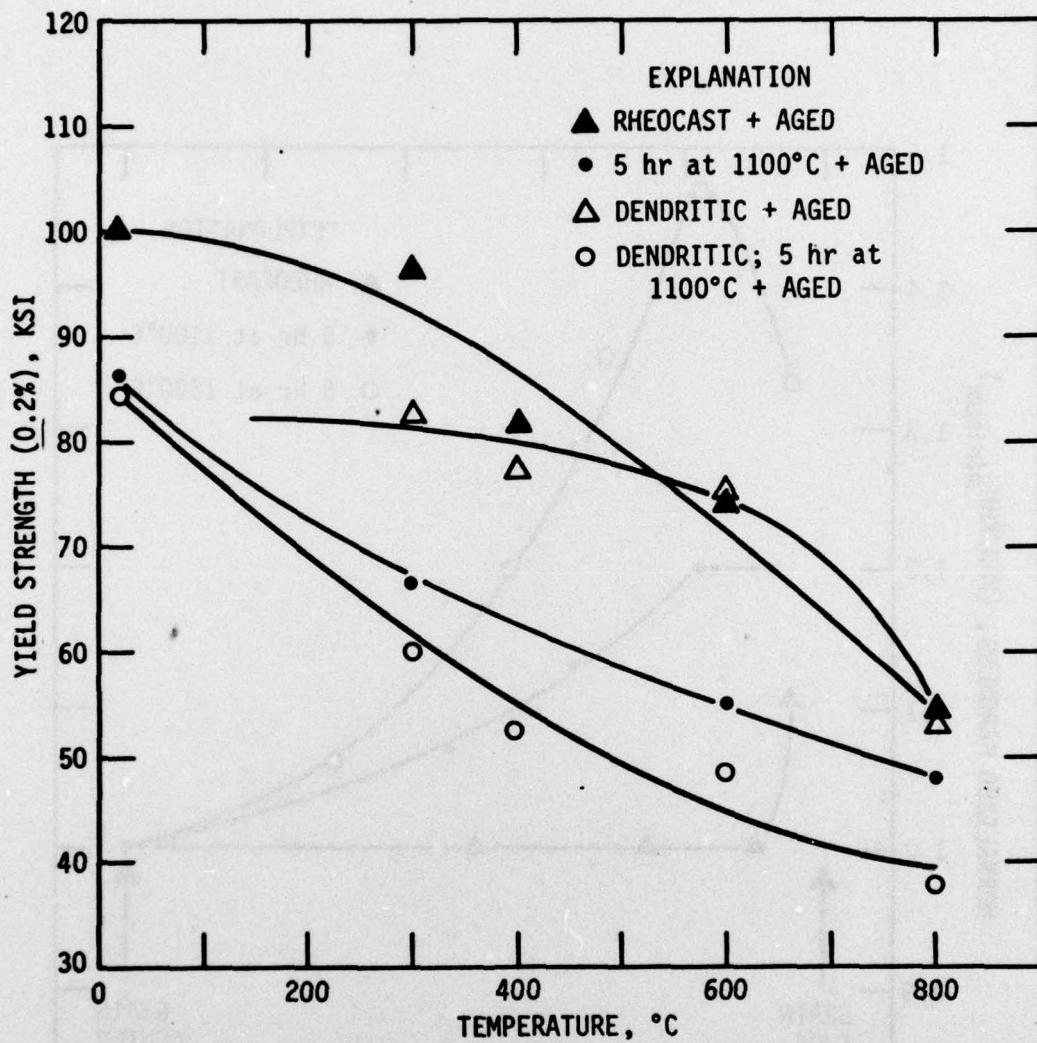
Figure 20 Measured compressive yield strength for dendritic and Rheocast X-40 cobalt base superalloy after two different heat treatments. (1) Aged at 700°C for 50 hours; (2) homogenized (5 hours at 1100°C) plus aging at 700°C for 50 hours.
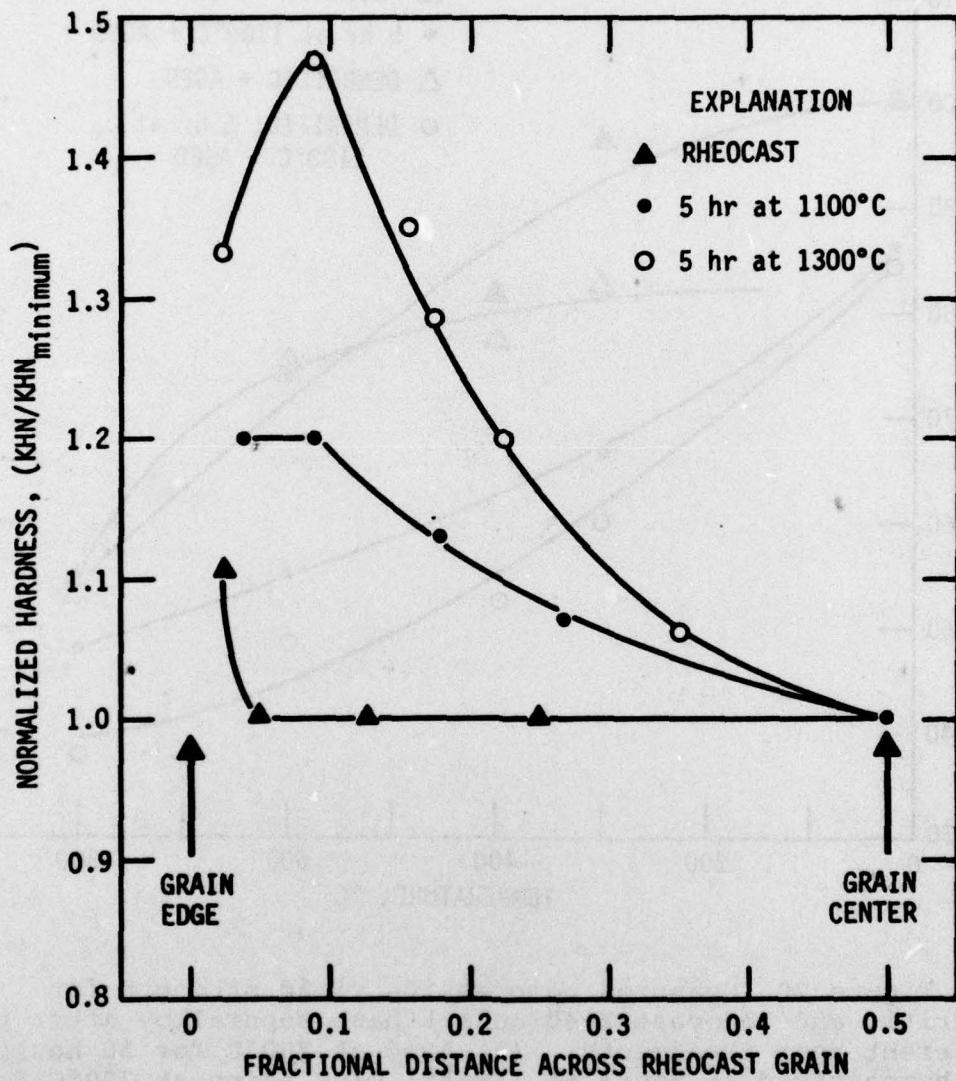
Figure 21 Measured variation of microhardness, normalized as the ratio of Knoop hardness number at a given location against the minimum value, across the Rheocast grain of X-40 cobalt base alloy in as-Rheocast and homogenized heat treated conditions.

DISTRIBUTION LIST

No. of Copies	To
1	Office of the Director, Defense Research and Engineering, The Pentagon, Washington, D. C. 20301
12	Commander, Defense Documentation Center, Cameron Station, Building 5, 5010 Duke Street, Alexandria, Virginia 22314
1	Metals and Ceramics Information Center, Battelle Columbus Laboratories, 505 King Avenue, Columbus, Ohio 43201

Chief of Research and Development, Department of the Army, Washington, D. C. 20310
2 ATTN: Physical and Engineering Sciences Division

Commander, Army Research Office, P. O. Box 12211, Research Triangle Park, North Carolina 27709
1 ATTN: Information Processing Office

Commander, U. S. Army Materiel Development and Readiness Command, 5001 Eisenhower Avenue, Alexandria, Virginia 22333
1 ATTN: DRCDE-TC

Commander, U. S. Army Electronics Command, Fort Monmouth, New Jersey 07703
1 ATTN: DRSEL-GG-DD
1   DRSEL-GG-DM

Commander, U. S. Army Missile Command, Redstone Arsenal, Alabama 35809
1 ATTN: Technical Library
1   DRSMI-RSM, Mr. E. J. Wheelahan

Commander, U. S. Army Armament Command, Rock Island, Illinois 61201
2 ATTN: Technical Library
1   DRSAR-SC, Dr. C. M. Hudson
1   DRSAR-PPW-PB, Mr. Francis X. Walter

Commander, U. S. Army Tank-Automotive Research and Development Command, Warren, Michigan 48090
2 ATTN: DRDTA, Research Library Branch

Commander, White Sands Missile Range, New Mexico 88002
1 ATTN: STEWS-WS-VT

Commander, Aberdeen Proving Ground, Maryland 21005
1 ATTN: STEAP-TL, Bldg. 305

Commander, Frankford Arsenal, Philadelphia, Pennsylvania 19137
1 ATTN: Library, H1300, Bl. 51-2
1   SARFA-L300, Mr. J. Corrie

No. of Copies	To

Commander, Picatinny Arsenal, Dover, New Jersey 07801
1 ATTN: SARPA-RT-S

Commander, Redstone Scientific Information Center, U. S. Army Missile
Command, Redstone Arsenal, Alabama 35809
4 ATTN: DRSMI-RBLD, Document Section

Commander, Watervliet Arsenal, Watervliet, New York 12189
1 ATTN: SARWV-RDT, Technical Information Services Office

Commander, U. S. Army Foreign Science and Technology Center,
220 7th Street, N. E., Charlottesville, Virginia 22901
1 ATTN: DRXST-SD2

Director, Eustis Directorate, U. S. Army Air Mobility Research and
Development Laboratory, Fort Eustis, Virginia 23604
1 ATTN: Mr. J. Robinson, SAVDL-EU-SS

Librarian, U. S. Army Aviation School Library, Fort Rucker, Alabama 36360
1 ATTN: Building 5907

Naval Research Laboratory, Washington, D. C. 20375
1 ATTN: Dr. J. M. Krafft - Code 8430

Chief of Naval Research, Arlington, Virginia 22217
1 ATTN: Code 471

Air Force Materials Laboratory, Wright-Patterson Air Force Base, Ohio 45433
2 ATTN: AFML/MXE/E. Morrissey
1   AFML/LC
1   AFML/LLP/D. M. Forney, Jr.
1   AFML/MBC/Mr. Stanley Schulman

National Aeronautics and Space Administration, Washington, D. C. 20546
1 ATTN: Mr. B. G. Achhammer
1   Mr. G. C. Deutsch - Code RR-1

National Aeronautics and Space Administration, Marshall Space Flight
Center, Huntsville, Alabama 35812
1 ATTN: R-P&VE-M, R. J. Schwinghamer
1   S&E-ME-MM, Mr. W. A. Wilson, Building 4720

Wyman-Gordon Company, Worcester, Massachusetts 01601
1 ATTN: Technical Library

Defense Advanced Research Projects Agency, 1400 Wilson Boulevard,
Arlington, Virginia 22209
5 ATTN: Dr. E. C. van Reuth

2

No. of Copies	To
	National Science Foundation, 1800 G Street, Washington, D. C. 20550
1	ATTN: Dr. Robert Reynik
	General Electric Company, Corporate Research and Development, Schenectady, New York 12301
5	ATTN: Mr. F. X. Gigliotti, Jr.
	Hitchiner Manufacturing Co., Inc., Elm Street, Milford, New Hampshire 03055
5	ATTN: Mr. G. D. Chandley
	Abex Corporation, Research Center, Mahwah, New Jersey 07430
5	ATTN: H. R. Larson
	Massachusetts Institute of Technology, Dept. of Metallurgy and Materials Science, Cambridge, Massachusetts 02139
1	ATTN: Dr. Merton C. Fleming
	TRW Equipment, TRW Inc., 23555 Euclid Avenue, Cleveland, Ohio 44117
1	ATTN: Elizabeth Barrett, T/M 3417
	Deposits & Composites Inc., 1821 Michael Faraday Drive, Reston, Virginia 22090
1	ATTN: Richard E. Engdahl, President
1	Dr. Maurice Sinnott, University of Michigan, Assoc. Dir. of Engineering, Ann Arbor, Michigan 48104
1	Fred E. Ziter, Adirondack Steel Casting Co., Shaker Road, Watervliet, New York 12189
1	Dr. Raymond J. Bratton, Westinghouse Electric Corporation Research Laboratory, Pittsburgh, Pennsylvania 15235
1	W. M. Spurgeon, Director, Mfg., Quality Control & Home Systems, Program Management Center, Bendix Research Laboratories, Bendix Center, Southfield, Michigan 48075
1	S. T. Wlodek, Director of Stellite R&D, Stellite Division, Cabot Corporation, 1020 West Park Avenue, Kokomo, Indiana 46901
1	Mr. William A. Butler, Contract Administrator, Microwave Associates, Inc., Burlington, Massachusetts 01803
1	Mr. John A. Ulrich, Sr. Vice-President, Chamberlain Manufacturing Corp., Waterloo, Iowa 50705
1	A. V. Illyn, Technical Director, Babcock & Wilcox, Old Savannah Road, Augusta, Georgia 30903

No. of Copies	To

1 Mr. W. J. Welsch (Code 224), Naval Materials Industry Resources Office, N.A.E.C., Building #537, Philadelphia, Pennsylvania 19112

1 Mr. R. E. Cross, Federal Die Casting Co., 2222 Elston Avenue, Chicago, Illinois 60614

1 Captain Ebenezer F. Porter, 2618 S. Lynn Street, Arlington, Virginia 22202

1 Mr. Charles E. Bates, Head, Metallurgy Section, Southern Research Institute, 2000 Ninth Avenue, South, Birmingham, Alabama 35205

1 Mr. R. F. Kirby, Chief, Materials Engineering Dept., Dept. 93-39M, Airesearch Manufacturing Company of Arizona, 402 South 36th Street, P. O. Box 5217, Phoenix, Arizona 85010

1 Dr. Mervin T. Rowley, American Foundry Men's Society, Golf & Wolf Roads, Des Plaines, Illinois 60016

1 William R. Freeman, Jr., Howmet Corporation, Vice President and Technical Director, Technical Center, Gas Turbine Components Group, 699 Benston Road, Whitehall, Michigan 49461

1 Dole A. Marek, General Motors Corporation, Detroit Diesel Allison, 4700 W 10th Street, Indianapolis, Indiana 46206

General Dynamics, Convair Aerospace Division, P. O. Box 748, Ft. Worth, Texas 76101
1 ATTN: Mfg. Engineering Technical Library

1 Dr. Robert Mehrabian, Dept. of Metallurgy & Mining Engineering, University of Illinois, Urbana, Illinois 61801

1 Robert McNally, Research Library, Special Metals Corporation, Middle Settlement Road, New Hartford, New York 13413

Director, Army Materials and Mechanics Research Center, Watertown, Massachusetts 02172
2 ATTN: DRXMR-PL
1 DRXMR-PR
1 DRXMR-AP
1 DRXMR-CT
1 DRXMR-X
1 DRXMR-ER

4

REPORT DOCUMENTATION PAGE		READ INSTRUCTIONS BEFORE COMPLETING FORM
1. REPORT NUMBER AMMRC CTR-77-26	2. GOVT ACCESSION NO.	3. RECIPIENT'S CATALOG NUMBER
4. TITLE (and Subtitle) MACHINE CASTING OF FERROUS ALLOYS.		5. TYPE OF REPORT & PERIOD COVERED Semi-Annual Report. no.3 1 Oct 76 — 31 Nov 77. 6. PERFORMING ORG. REPORT NUMBER
7. AUTHOR(s) R./Mehrabian, D.G./Backman, G.J./Abbaschian, Y.V./Murty S.D.E./Ramati		8. CONTRACT OR GRANT NUMBER(s) DAAG46-76-C-0023, ARPA Order-2267
9. PERFORMING ORGANIZATION NAME AND ADDRESS		10. PROGRAM ELEMENT, PROJECT, TASK AREA & WORK UNIT NUMBERS D/A Project: 2267 AMCMS Code: 6Y10 Agency Accession:
11. CONTROLLING OFFICE NAME AND ADDRESS Army Materials and Mechanics Research Center Watertown, Massachusetts 02172		12. REPORT DATE October 1977 13. NUMBER OF PAGES 42
14. MONITORING AGENCY NAME & ADDRESS(if different from Controlling Office)		15. SECURITY CLASS. (of this report) Unclassified
		15a. DECLASSIFICATION/DOWNGRADING SCHEDULE

16. DISTRIBUTION STATEMENT (of this Report)

Approved for public release; distribution unlimited.

17. DISTRIBUTION STATEMENT (of the abstract entered in Block 20, if different from Report)

18. SUPPLEMENTARY NOTES

19. KEY WORDS (Continue on reverse side if necessary and identify by block number)

Die Casting
Solidification
Ferrous alloys

20. ABSTRACT (Continue on reverse side if necessary and identify by block number)

This is the third semi-annual report describing research conducted at the University of Illinois at Urbana-Champaign as part of a joint university-industry research program on machine casting of ferrous alloys. It covers a period of six months, 1 October 1976 to 31 March 1977. The work at the University of Illinois was initiated on 1 October 1975 at which time the overall program had already been in effect for 33

DD FORM 1473 EDITION OF 1 NOV 65 IS OBSOLETE
1 JAN 73

months.

This report covers work carried out in the past six months and summarizes results to date in two areas of this investigation. These include the following:

1. A summary of all the findings to date on the relationship between process variables and Rheocast structures produced in a low-temperature continuous slurry producer and

2. The effect of cast (Rheocast) structure on microsegregation, homogenization heat treatment response, and mechanical properties of high-temperature alloys.

The three important process variables affecting structure and viscosity of a continuously produced Sn-15% Pb alloy slurry are average shear and cooling rates during primary solidification and volume fraction solid in the slurry. Increasing the average cooling rate makes the primarily solid particles smaller and more uniform in size but increases the amount of entrapped liquid in each particle. Increasing the average shear rate affects particle size and uniformity of size similarly, except this effect is noted only at low cooling rates. Primary solid particle size in a vigorously agitated slurry is approximately the same as primary dendrite arm spacing in a conventional casting solidified at equivalent cooling rate. As the volume fraction solid in a slurry increases, so does it primary solid particle size and hence viscosity.

Work on three high-temperature alloys, 905 copper base alloy, 440C stainless steel, and X-40 cobalt base superalloy, shows that Rheocast materials

1. Have a microsegregation pattern that is slightly different from conventionally solidified dendritic structures,

2. Respond to homogenization heat treatment, and

3. In the absence of porosity, possess mechanical properties comparable to conventional castings.

Army Materials and Mechanics Research Center
Watertown, Massachusetts 02172
MACHINE CASTING OF FERROUS ALLOYS
R. Mehrabian, D.G. Backman, Y.V. Murty,
G.J. Abbaschian, S.D.E. Ramati

AD _____
UNCLASSIFIED
UNLIMITED DISTRIBUTION

Key Words

Die Casting
Solidification
Ferrous Alloys

Semi-Annual Report AMMRC CTR 77-26, October 1977
42 pp - illustrations, D/A Project ARPA
Order No. 2267, AMCMS Code 6Y10

This is the third semi-annual report describing research conducted at the University of Illinois at Urbana-Champaign as part of a joint university-industry research program on machine casting of ferrous alloys. It covers a period of six months, 1 October 1976 to 31 March 1977. The work at the University of Illinois was initiated on 1 October 1975 at which time the overall program had already been in effect for 33 months. This report covers work carried out in the past six months and summarizes results to date in two areas of this investigation. These include the following: (1) A summary of all the findings to date on the relationship between process variables and Rheocast structures produced in a low-temperature continuous slurry producer and (2) The effect of cast (Rheocast) structure on microsegregation, homogenization heat treatment response, and mechanical properties of high-temperature alloys.

Army Materials and Mechanics Research Center
Watertown, Massachusetts 02172
MACHINE CASTING OF FERROUS ALLOYS
R. Mehrabian, D.G. Backman, Y.V. Murty,
G.J. Abbaschian, S.D.E. Ramati

AD _____
UNCLASSIFIED
UNLIMITED DISTRIBUTION

Key Words

Die Casting
Solidification
Ferrous Alloys

Semi-Annual Report AMMRC CTR 77-26, October 1977
42 pp - illustrations, D/A Project ARPA
Order No. 2267, AMCMS Code 6Y10

This is the third semi-annual report describing research conducted at the University of Illinois at Urbana-Champaign as part of a joint university-industry research program on machine casting of ferrous alloys. It covers a period of six months, 1 October 1976 to 31 March 1977. The work at the University of Illinois was initiated on 1 October 1975 at which time the overall program had already been in effect for 33 months. This report covers work carried out in the past six months and summarizes results to date in two areas of this investigation. These include the following: (1) A summary of all the findings to date on the relationship between process variables and Rheocast structures produced in a low-temperature continuous slurry producer and (2) The effect of cast (Rheocast) structure on microsegregation, homogenization heat treatment response, and mechanical properties of high-temperature alloys.